



1 **Annual variability and regulation of methane and sulfate fluxes in**
2 **Baltic Sea estuarine sediments**

3

4

5

6

Joanna E. Sawicka and Volker Brüchert

7

8

9

10 Department of Geological Sciences, Stockholm University, Stockholm, 10691, Sweden

11

12

13 *Correspondence to:* Volker Brüchert (volker.bruchert@geo.su.se)

14

15

16

17

18

19

20

21

22

23

24

25

26

27

28

29



30 **Abstract.** The effects of temperature, changes in benthic oxygen concentration, and historical
31 eutrophication on sediment methane concentrations and benthic fluxes were investigated at two type
32 localities for open-water coastal and eutrophic, estuarine sediment in the Baltic Sea. Benthic fluxes of
33 methane and oxygen, sediment porewater concentrations of dissolved sulfate, methane, and ^{35}S -sulfate
34 reduction rates were obtained over a 12-month period from April 2012 to April 2013. Benthic methane
35 fluxes varied by factors of 5 and 12 at the offshore coastal site and the eutrophic estuarine station,
36 respectively, ranging from $0.1 \text{ mmol m}^{-2}\text{d}^{-1}$ in winter at an open coastal site to $2.6 \text{ mmol m}^{-2}\text{d}^{-1}$ in late
37 summer in the inner eutrophic estuary. Total oxygen uptake (TOU) and ^{35}S -sulfate reduction rates
38 (SRR) correlated with methane fluxes showing low rates in the winter and high rates in the summer.
39 The highest porewater methane concentrations also varied by factors of 6 and 10 over the sampling
40 period with lowest values in the winter and highest values in late summer-early autumn. The highest
41 porewater methane concentrations exceeded 6 mM a few centimeters below the sediment surface, but
42 never exceeded the in-situ saturation concentration. 21 – 24% of the total sulfate reduction was coupled
43 to anaerobic methane oxidation lowering methane concentrations below the sediment surface far below
44 the saturation concentration. These data imply that bubble emission likely plays no or only a minor role
45 for methane emissions in these sediments. The changes in porewater methane concentrations over the
46 observation period are too large to be explained by temporal changes in methane formation and
47 methane oxidation rates. Instead, it appears that advective methane recharge supplies of methane from
48 deeper sediment layers to near-surface sediment. These are possible related to the transport of methane
49 from deeper gas-rich areas or due to free gas movement or groundwater discharge.

50

51

52

53 **Keywords** Methane, sulfate reduction, estuary



54 **1 Introduction**

55 The world's estuaries have been estimated to emit between 1.8 and 6.6 Tg CH₄ y⁻¹ to the atmosphere
56 (Borges and Abril, 2011; Amouroux et al 2002, Marty et al., 2001; Middelburg et al., 2002; Sansone et
57 al., 1999; Upstill-Goddard et al., 2000). As other globally upscaled estimates of emissions, these
58 estimates also have considerable uncertainties. In the case of estuaries, a major cause of the uncertainty
59 are relatively few spatially and temporally resolved measurements of anaerobic carbon degradation
60 measurements in sediments and measurements of methane fluxes from sediments. In estuarine waters
61 methane is produced by methanogenesis in underlying anoxic sediments, lateral freshwater or sewage
62 discharge, seepage of methane-rich groundwater, or transport in the near-shore by aquatic plants
63 (Borges and Abril, 2011). The amount of sedimentary methane production in estuaries is a function of
64 organic matter availability, bottom water oxygen concentrations, and the salinity of the estuary.
65 Methane production is generally greater in low-salinity estuaries because of lower sulfate availability to
66 promote bacterial sulfate reduction (Borges and Abril, 2011). Methane fluxes from estuarine sediments
67 are characterized by significant spatial and temporal variability (Borges and Abril 2011). Temporal
68 patterns show that concentrations and fluxes of CH₄ are generally higher in the warmer summer season
69 and low in the colder season (Crill et al., 1983, Martens and Klump, 1984, Musenze et al., 2014; Reindl
70 and Bolalek, 2014). Notably, very few studies have considered CH₄ fluxes during snow- and ice-
71 covered periods. While shallow systems within the tidal range derive a significant amount of the
72 methane flux from ebullition (Martens and Klump, 1984), groundwater discharge, tidal pumping, and
73 transport by aquatic plants (Middelburg et al., 2002; Kristensen et al 2008), the transport from deeper
74 systems such as fjords and fjärds is thought to occur largely by molecular diffusion (Abril and Iversen,
75 2002, Sansone et al., 1998).

76 Globally more than 90% of methane produced in marine sediments is estimated to be oxidized by the
77 anaerobic oxidation of methane (AOM), mostly in the sulfate-methane transition zone (Knittel and
78 Boetius, 2009, Martens and Berner, 1974; Jørgensen and Parkes, 2010). It is not known how much



79 methane is oxidized by AOM in estuarine sediments. In addition, up to 90% of the remaining methane
80 that reaches the sediment surface may be oxidized aerobically at the sediment surface or in the water
81 column (Reeburgh, 2007). Yet, methane concentrations in estuarine waters are almost always higher
82 than the atmospheric equilibrium concentration indicating that microbial oxidation processes and
83 physical exchange with the atmosphere in estuaries are relatively inefficient in removing methane.

84 Despite its obvious importance, only few studies have specifically addressed anaerobic oxidation of
85 methane by sulfate and aerobic oxidation in estuarine environments (e.g., Treude et al., 2005, Thang et
86 al., 2013). The aim of this study was to further elucidate mechanisms behind temporal variability of
87 methane fluxes in a high-latitude coastal and estuarine environment with winter ice cover. We
88 determined porewater concentrations of methane and sulfate, measured sulfate reduction rates with the
89 ^{35}S -sulfate tracer method, and conducted core incubations to determine benthic fluxes of methane and
90 oxygen at two deep stations of a low-salinity Baltic Sea estuary inside and at the opening of the estuary
91 to the Baltic. Investigations were carried out over four seasons to capture the annual variability of
92 chemical and biological conditions at the sediment surface and their influence on methane dynamics.

93

94 **2 Materials and methods**

95 **2.1 Site description**

96 Himmerfjärden (Figure 1) is a fjord-type estuary with a surface area of 174 km^2 and a N-S
97 salinity gradient increasing from 5.5‰ in the inner part to 7.0‰ at the opening to the Baltic. It is
98 morphologically characterized by four basins, divided by sills. Water discharge to the estuary is low
99 (flushing rate 0.025/day) and derives from land run-off and precipitation (33% and 14% respectively),
100 outflow from Lake Mälaren in the north (46%), discharge of a major sewage treatment plant (STP)
101 (7%) (Boesch et al., 2006; Engqvist, 1996). The STP, built in the early 1970s, treats sewage water from
102 300,000 inhabitants of the southern Stockholm metropolitan area, and its inorganic effluent is
103 discharged mainly in the form of inorganic nitrogen and phosphorus to the inner basins (Savage and



104 Elmgren, 2010). The estuary undergoes thermohaline stratification during late summer and autumn,
105 especially in the inner part, which experiences regular seasonal bottom water hypoxia. The tidal range
106 is low (few cm) and relatively cold bottom waters (1.5 - 9°C) dominate throughout the year. Late-
107 summer-early fall bottom water hypoxia has also been reported occasionally for the outer basins of the
108 estuary when winds are weak and circulation is inhibited (Elmgren and Larsson, 1997).

109 Bottom water and sediment samples were taken from a station in the inner part of
110 Himmerfjärden, Station H6, and from a station located outside the estuary, Station B1 (Figure 1).
111 Samples were collected in April, August, October 2012, and in February 2013. In addition, in April
112 2013 whole-core incubations were performed to determine methane and oxygen fluxes to record a full
113 year of seasonal variability. Station B1 has soft, olive grey, muddy sediment with a rusty brown surface
114 layer, while the sediment at station H6 is soft, laminated black mud with a 1-2 mm thin brown surface
115 layer that occurs during the winter and spring. Sediment accumulation rates range from 0.98 cm yr⁻¹ in
116 the innermost part of the estuary to 0.77 cm yr⁻¹ in the outer part of the estuary (Thang et al., 2013).

117

118 2.2 Sample collection

119 Sediments with well-preserved sediment surfaces were collected with a Multicorer in acrylic tubes (9.5
120 cm diameter) to 40 cm depth to determine ³⁵S-sulfate reduction rates, porosity, and the porewater
121 constituents methane and sulfate. Additional cores were collected for sediment core incubations.
122 Porewater methane samples were immediately collected on-board from the cores as described below.
123 The other cores were capped with rubber stoppers, transported to the marine laboratory on the island of
124 Askö within 90 minutes and kept cold at bottom water temperatures for later experiments and
125 subsampling. In February 2013, ice partially covered Station B1 and there was full ice coverage at
126 Station H6, and sampling was only possible after ice breaking. For whole-core incubations, 30 l of
127 bottom water was collected with a 5 liter HydroBios bottle and kept cold until for the experiments.
128 Temperature, salinity, and oxygen concentrations were determined with a handheld WTW Oxygen
129 meter directly in the water overlying the sediment cores.



130

131 2.3 Organic carbon concentrations and porosity

132 Surface sediment concentrations of organic carbon were determined on freeze-dried sediment with a
133 Fisons CHN elemental analyzer after treatment of freeze-dried sediment with 1N HCl to remove
134 inorganic carbon. Water content (%) was determined by drying 5 ml of sediment at 105°C for two
135 hours and calculating the percent loss after drying.

136

137 2.4 Methane analysis

138 Samples for methane were collected directly through the side of taped, pre-drilled core liners and taken
139 in 2-cm intervals seconds after the core was retrieved on deck. The core sampling method used in this
140 study permits complete sampling and preservation of porewater methane within 5 minutes after the
141 core was on deck. Under these circumstances, loss of methane due to gas loss is low and methane
142 concentrations could be determined for porewaters that were far above the saturation limit at 1
143 atmosphere pressure for the salinity and temperature range of the bottom water (between 1.9 mM and
144 2.4 mM). A sediment sample of exactly 2.5 mL was taken with a 3 mL cutoff syringe. The sample was
145 transferred to a 20 mL serum vial containing 5 mL 5 M NaCl and immediately closed with a thick
146 septum and an aluminum crimp seal. The sample was shaken, left for 1 hour for gas equilibration, and 5
147 mL of brine was injected into a sample vial to force out the 5 mL gas samples out of a vial into the
148 syringe. The CH₄ measurements were carried out on a gas chromatograph (GC) with a flame ionization
149 detector (FID) (SRI 8610C) and N₂ was used as carrier gas. CH₄ standards 100 ppm and 10000 ppm
150 (Air Liquide) were used for calibration.

151 The concentration of methane (mM) in the headspace of a sample was calculated from:

$$152 \quad CH_4(mM) = \frac{V_{headspace} A \alpha}{24.1 V_{sediment} \rho} \quad (1)$$

153



154 where V_{head} is the volume of the headspace in the sample vial (cm^3), ρ is the sediment porosity, A is the
155 peak area of methane eluted, α is the slope of the standard curve (parts per million volume basis), and
156 V_{sed} is the volume of the sediment sample (cubic centimeter). The molar volume of methane at 20°C
157 and 1 atm pressure (24.148 L mol^{-1}) was used to convert from partial volume of CH_4 gas to the mole
158 fraction of CH_4 .

159

160 **2.5 Sulfate concentration**

161 Porewater samples for sulfate concentration measurements were obtained using rhizones (Atlas
162 Copco Welltech) (Seeberg-Elverfeldt et al 2005). Rhizones were treated for 2 hours in 10% HCl
163 solution, followed by two rinses with deionized water for 2 hours and final storage in deionized water.
164 Rhizones were connected to 10 mL disposable plastic syringes via a 3-way luer-type stop-cock and
165 inserted in 1 cm intervals through tight-fitting, pre-drilled holes in the liner of the sediment cores. The
166 first mL of pore water was discarded from the syringe. No more than 2 ml were collected from each
167 core to prevent cross-contamination of adjacent due to the porewater suction (Seeberg-Elverfeldt et al.,
168 2005). Sulfate concentration was measured on a Dionex System IC 20 ion chromatograph.

169

170 **2.6 ^{35}S -Sulfate reduction rates**

171 To determine bacterial sulfate reduction rates (SRR) sediment cores were subsampled in 40-cm
172 long 28 mm-diameter cores with 1-cm spaced, silicon-sealed, pre-drilled small holes on the side for
173 injections. For the incubation, the whole-core incubation method by Jørgensen (1978) was used. $^{35}\text{SO}_4^{2-}$
174 tracer solution was diluted in a 6 % NaCl solution containing 0.5 mM SO_4^{2-} and 2.5 μl of the tracer
175 solution (50kBq) was injected through the pre-drilled holes. The cores were then capped and sealed in
176 plastic wrap foil and incubated for 8 hours at the respective bottom water temperatures. After this time,
177 the incubations were stopped by sectioning the core in 1-cm intervals to 5 cm depth and in two
178 centimeter intervals below this depth to the bottom of the core. Sediment sections were transferred into
179 50 ml plastic centrifuge tubes containing 20 ml zinc acetate (20% v/v) and shaken vigorously and



180 frozen. The total amount of ^{35}S -labeled reduced inorganic sulfur (TRS) was determined using the
181 single-step cold distillation method by Kallmeyer et al. (2004). TRS and supernatant sulfate were
182 counted on a TriCarb 2095 Perkin Elmer scintillation counter. The sulfate reduction rate was calculated
183 using the following equation (Jørgensen, 1978):

$$184 \quad {}^{35}\text{SRR} = \frac{\text{TRI}^{35}\text{S} \rho 1.06}{({}^{35}\text{SO}_4^{2-} + \text{TRI}^{35}\text{S}) T} \quad (2)$$

185 where $(\text{SO}_4^{2-} \rho)$ is the pore water sulfate concentration corrected for porosity ρ , TRI^{35}S and ${}^{35}\text{SO}_4^{2-}$ are
186 the measured counts (cpm) of sulfate and total reduced sulfur species, respectively, 1.06 is a correction
187 factor accounting for the isotope discrimination of ^{35}S against ^{32}S -sulfate, and T is the incubation time.
188 The sulfate reduction rate is reported as $\text{nmol cm}^{-3} \text{day}^{-1}$. ${}^{35}\text{SRR}$ were measured in three parallels cores
189 for all depth intervals and the values reported here are the median values of the triplicates. The
190 detection limit of the rate measurements accounting for distillation blanks and radioactive decay of ${}^{35}\text{S}$
191 between experiment and laboratory workup was $0.1 \text{ nmol day}^{-1} \text{ cm}^{-3}$.

192

193 **2.7 Whole-core sediment incubations**

194 Four intact cores with undisturbed sediment surfaces and clear overlying water were subsampled in the
195 laboratory in acrylic tubes (i.d. 6.2 cm, height 25 cm) retaining about 10 cm of the overlying water. The
196 sediment height in the tubes was approximately 10 cm. The cores were incubated in a 40-liter
197 incubation tank filled with bottom water from the same station. Before the incubation the overlying
198 water in the cores was equilibrated with bottom water in the tank. The overlying water in the cores was
199 stirred by small magnetic bars mounted in the core liners and driven by an external magnet at 60 rpm.
200 The cores were pre-incubated uncapped for 6 hours and subsequently capped and incubated for a period
201 of 6 to 12 hours depending on the initial oxygen concentration in the bottom water.

202



203 **2.8 Total oxygen uptake**

204 Oxygen sensor spots (Firesting oxygen optode, PyroScience GmbH, Germany) with a sensing surface
205 of a diameter of 5 mm were attached to the inner wall of two incubation cores (diameter 5.5 cm). The
206 sensor spots were calibrated against O₂-saturated bottom water and oxygen-free water following the
207 manufacturer's guidelines accounting for temperature and salinity of the incubation water.
208 Measurements were performed with a fiberoptic cable connected to a spot adapter fixed at the outer
209 core liner wall at the spot position. The O₂ concentration was continuously logged during incubations.
210 Sediment total oxygen uptake (TOU) rates were computed by linear regression of the O₂ concentration
211 over time.

212

213 **2.9 Methane fluxes**

214 Methane fluxes were determined from discrete water samples collected in 12 mL Exetainers (Labco,
215 Wycombe, UK) prefilled with 50 µL of 50% ZnCl₂ without headspace. Samples were collected at the
216 beginning (time zero) and at the end of the incubation (time final), usually after 24 hours. CH₄
217 concentrations were determined using the headspace equilibration technique (Kampbell et al., 1989) by
218 displacing 3 ml of the water in the exetainers with high-purity helium gas at atmospheric pressure. The
219 Exetainers were shaken at 400rpm on a shaking table for 60 minutes to allow the gas to equilibrate
220 between the headspace and the liquid phase and left to rest for half an hour. After equilibration 2.5 mL
221 of NaCl brine was injected into an Exetainer to force the gas samples into an injection syringe while
222 maintaining the headspace pressure. The samples were injected onto a 1 ml injection loop of a gas
223 chromatograph (SRI 8610) with FID detector using N₂ as carrier gas. CH₄ standards 5 ppm, 100 ppm
224 and 10000 ppm (Air Liquide) were used to construct a calibration curve.
225 Partial pressure of CH₄ in the equilibrated headspace and water was calculated using the solubility
226 coefficient β for CH₄ (Wilhelm et al 1977), gas constant R (8.314 L kPa mol⁻¹ K⁻¹), air pressure (P in



227 kPa), headspace gas concentration CH_4 (hsp) (ppm), headspace volume (0.003L), water volume in the
 228 extainer (0.009L), and laboratory temperature (293 K) according to

$$229 \quad \text{CH}_4 \text{ (nM)} = (\text{CH}_4 \text{ (hsp)} + \beta \text{ CH}_4 \text{ hsp}) * P/RT \quad (3)$$

230 Fluxes (J) of CH_4 ($\text{mmol m}^{-2} \text{ d}^{-1}$) during the whole core sediment incubations were calculated according
 231 to

$$232 \quad J = (\text{CH}_4 \text{ start} - \text{CH}_4 \text{ end})/T * V/A \quad (4)$$

233 where $\text{CH}_4 \text{ start}$ and $\text{CH}_4 \text{ final}$ represent the end and start concentrations in mmol/m^3 , V is headspace
 234 volume (L), A is the surface area of the incubation core (m^2), and T is the incubation time (days).

235

236 **2.10 Diffusive flux calculations**

237 Diffusive fluxes of methane and sulfate were estimated from the porewater gradients of methane and
 238 sulfate for the sediment surface and the sulfate-methane transition zone. Sediment cores at station B1
 239 showed occasional burrows from deposit feeders in the topmost 2 cm of sediment, whereas sediment at
 240 station H6 was largely devoid of macro- and meiofauna. Since only one sample was taken from the
 241 topmost 2 cm, quantitative depth-related effects of bioturbation cannot be accounted for in this analysis
 242 and upward diffusive transport of methane was assumed as the dominant transport pathway. Fluxes
 243 were estimated using Fick's first law of diffusion

$$244 \quad J = D_s \frac{dc}{dx} \quad (5)$$

245 assuming that flux was dominated by molecular diffusion, where dC is the change in concentration of
 246 dissolved sulfate (mM) or methane (mM) over a depth interval dx (cm), and D_s is the sediment
 247 diffusion coefficient corrected for temperature and salinity according to Boudreau (1996). D_s was
 248 recalculated from the molecular diffusion coefficient D_o for sulfate and methane according to Iversen
 249 and Jørgensen (1994).

250



251 **3 Results**

252 **3.1 Bottom water temperature, dissolved oxygen, organic carbon**

253 During the observation period April 2012 through February 2013 salinity varied between 5.4 and 6.5‰
254 at Station H6 and 6.5 and 7.0‰ at station B1 (Table 1), while bottom water temperatures ranged from
255 2.4°C to 6.9°C at station B1 and 1.8°C to 9.4°C at station H6. The lowest and highest bottom water
256 oxygen concentrations were measured in April 2012 (40 µM at station H6, and 160 µM at station B1)
257 and February 2013 (300 at station H6 and 380 µM at station B1, respectively). Surface sediment
258 organic carbon concentrations were similar at the two stations ranging between 4.6 and 5.2% at Station
259 B1, and 5.0% and 6.0% at Station H6.

260

261 **3.2 Methane and sulfate concentrations**

262 The highest methane concentrations in the sediment cores were recorded in August, when they reached
263 5.7 mM at station H6 and 1.9 mM at station B1 (Figure 2a-h). Methane concentrations were lowest in
264 February, when the highest concentrations in the cored sediment were 1.5 mM at station H6 and only
265 0.1 mM at station B1. The measured methane concentrations never exceeded the solubility limit for
266 methane calculated for the *in situ* pressure, which ranged from 9.6 to 11.9 mM during the different
267 sampling periods. Generally, methane concentrations at station H6 increased linearly from the surface
268 down to 10 cm depth. Below this depth they only increased slightly or remained constant. An exception
269 to this trend was observed in February at station B1, when methane showed a concave-upward trend
270 indicating active consumption of methane in the topmost 10 cm of sediment.

271 Sulfate concentration gradients changed considerably between the different seasons at both stations
272 reflecting substantial changes in sulfate reduction rates over the observation period. At both stations,
273 the sulfate concentration gradients were steepest in October, intermediate in April and August, and
274 lowest in February indicating highest and lowest sulfate reduction rates in October and February,
275 respectively (Figure 3 a-h). At station H6, sulfate was always depleted in the cored sediment interval,



276 albeit at substantially greater depth in February. Depletion already occurred at 5 cm depth in April and
277 October and at 9 cm depth in August, and sulfate concentrations showed a typically concave downward
278 gradient. At station B1, sulfate was never consumed completely and concentrations remained above 1.5
279 mM at the bottom of the core. Generally, sulfate decreased steeply from the surface down to 10 cm
280 depth in August and October. Below this surface zone there was an interval with nearly constant
281 concentrations down to 20 cm depth, below which sulfate decreased again to a concentration to about
282 1.5 mM. Despite some variability in the sulfate concentration profiles and a lower gradient in the
283 topmost centimeters in April and February, the sulfate concentrations at the bottom of the core were
284 similar during all observation periods.

285

286 3.3 ³⁵S-sulfate reduction rates

287 In agreement with the sulfate concentration gradients, ³⁵S-sulfate reduction rates were higher at station
288 H6 than at station B1 (Figure 4 a-h). At station B1, SRR ranged from 0.2 nmol cm⁻³ d⁻¹ to 63 nmol cm⁻³
289 d⁻¹, while at H6 SRR were as high as 411 nmol cm⁻³ d⁻¹. Organoclastic sulfate reduction dominated the
290 interval down to 10 cm. Depth-integrated sulfate reduction rates over the core length varied from 9.2 to
291 11.7 mmol m⁻² d⁻¹ at station H6 and 0.5 to 2.4 mmol m⁻² d⁻¹ at station B1.

292 Two distinct sulfate reduction rate peaks were found at station H6, one at the surface and a second peak
293 between 10 cm and 15 cm depth. The latter is in the sulfate-methane transition zone and indicates that
294 in this depth interval the rates of anaerobic methane oxidation coupled to sulfate reduction exceeded
295 organoclastic sulfate reduction rates. Depth-integrated rates of sulfate reduction in the sulfate-methane
296 transition zone at H6 were relatively constant and varied between 2.4 mmol m⁻² d⁻¹ and 2.8 mmol m⁻² d⁻¹
297 (Table 2). In February, when sulfate penetrated to 24 cm depth, sulfate reduction rates were about two
298 times lower compared to the other months and a second sulfate reduction peak coupled to methane
299 oxidation was not visible. However, the distinct upward concave curvature of the methane profile in
300 February at station B1 indicates that even here some of sulfate reduction was coupled to anaerobic
301 methane oxidation and that this process overlapped with organoclastic sulfate reduction. Sulfate



302 reduction was also detected below the sulfate-methane transition zone at station H6 in April, August,
303 and October. Since non-radioactive carrier sulfate was added to the ^{35}S -tracer during these incubations,
304 these rates indicate potential sulfate reduction activity in the methanogenic zone (Leloup et al., 2009).
305 The lack of the second peak in February at H6 is in agreement with previous observations that
306 productive seasons lead to shoaling of the methane-dependent sulfate reduction activity and anaerobic
307 oxidation methane layer in the sediments (Dale et al 2008, Treude et al 2005a). Previous studies at
308 neighboring stations H2 and H3 found AOM present at the depths 6-16 cm and 16-28 respectively,
309 which is in agreement with our findings (Wegener et al 2012).

310

311 **3.4 Benthic exchange of oxygen, sulfate, and methane**

312 Rates of total oxygen uptake are summarized in Table 2 and shown for comparison in Figure 5. Total
313 oxygen uptake was lowest in February at both stations (B1: $-12 \pm 2.5 \text{ mmol m}^{-2} \text{ d}^{-1}$ and H6: -14.9 ± 3.5
314 $\text{mmol m}^{-2} \text{ d}^{-1}$) and highest in August at station H6 ($-26.9 \pm 3.7 \text{ mmol m}^{-2} \text{ d}^{-1}$) and in April at station B1 ($-$
315 $33.5 \pm 4.7 \text{ mmol m}^{-2} \text{ d}^{-1}$). The diffusive sulfate fluxes from the water column into the sediment ranged
316 from $-0.2 \text{ mmol m}^{-2} \text{ d}^{-1}$ in February to $-1.4 \text{ mmol m}^{-2} \text{ d}^{-1}$ in October at B1 and from $-1.3 \text{ mmol m}^{-2} \text{ d}^{-1}$ in
317 February to $-2.7 \text{ mmol m}^{-2} \text{ d}^{-1}$ in August at station H6 (Table 2). These rates are significantly lower
318 than the radiotracer rates and indicate that sulfate is reoxidized below the sediment surface by reaction
319 with reactive iron (Thang et al., 2013). Methane fluxes determined by whole-core incubation were
320 consistently higher than the fluxes determined from the concentration profiles of dissolved methane at
321 station H6, whereas the two methods gave similar results at Station B1 (Table 2). The seasonal
322 variability in fluxes at the two stations was similar for the two measuring methods (Table 2). Whole-
323 core methane fluxes ranged from $0.3 \text{ mmol m}^{-2} \text{ d}^{-1}$ (February) to $19.9 \text{ mmol m}^{-2} \text{ d}^{-1}$ (August) at station
324 H6, and from 0.1 (February and April) to $1.2 \text{ mmol m}^{-2} \text{ d}^{-1}$ (August) at station B1 (Figure 5, Table 2).
325 The very high value measured in August 2012 at Station H6 is likely due to ebullition during the
326 incubation at ambient air pressure. Diffusive methane fluxes ranged from $0.05 \text{ mmol m}^{-2} \text{ d}^{-1}$ to 1.6
327 $\text{mmol m}^{-2} \text{ d}^{-1}$ at Station B1 and from 0.4 to $2.6 \text{ mmol m}^{-2} \text{ d}^{-1}$ in August at H6. The good agreement



328 between whole-core fluxes and diffusion-based fluxes at station B1 suggests that bioturbation and
329 irrigation at this station had little influence on the methane exchange with the bottom water.

330

331 **4 Discussion**

332 **4.1 Bottom water temperature and salinity**

333 Correlations between biogeochemical rates and fluxes with bottom water temperatures in
334 Himmerfjärden between April 2012 and February 2013 were weak for the period April-October, and
335 forced by the low rates in the coldest observation period in early February 2013. The temperature
336 versus rate/flux relationships were generally non-linear and not consistent for the fluxes of oxygen,
337 methane, and sulfate indicating that additional controlling factors played a role. It is likely that the
338 microbial community involved in the cycling of methane and sulfur species in Himmerfjärden sediment
339 is temperature-sensitive, and that the low rates in February 2013 are due to the 3°C temperature drop in
340 bottom water from October 2012 to February 2013. This would be consistent with rate observations in
341 comparable environments by Treude et al (2005a), Abril and Iversen (2002), Crill and Martens (1983),
342 and Westrich and Berner (1988), and is also supported by studies of the microbial community
343 composition of estuarine sediments that showed variations as a function of temperature (e.g., Zhang et
344 al 2014). However, microbial community composition and biogeochemical rates often cannot be
345 directly established from binary relationships with temperature, since other physical and chemical
346 parameters such as salinity, bottom water oxygen concentrations, organic carbon accumulation also
347 vary seasonally. Of these, salinity is not considered to be important for the present study, because the
348 annual range in Himmerfjärden bottom water was only between 5.4 and 7 ‰, which is too small to
349 affect the major electron acceptor and carbon degradation pathways.

350



351 **4.2 Effects of organic matter composition and sedimentation**

352 Organic carbon concentrations in Himmerfjärden are comparable to other fjord- and fjärd-type
353 estuarine sediments (Bianchi, 2007; Smith et al., 2015). Primary organic carbon export in
354 Himmerfjärden varies strongly on both seasonal and interannual timescales. The major export periods
355 occur during the spring phytoplankton bloom in March-April to early May, a late-summer
356 cyanobacterial bloom in August, and a secondary phytoplankton bloom in September (Bianchi et al.,
357 2002; Zakrisson et al., 2014; Harvey et al., 2015). Terrestrial-derived organic carbon that is not derived
358 from the sewage treatment plant plays only a minor role in this system, because no major rivers enter
359 the system and surface rainwater runoff is low. Based on sediment trap studies, the annual organic
360 carbon flux in Himmerfjärden varies by more than an order of magnitude at station B1 and by about a
361 factor of 3 in the inner parts of Himmerfjärden (Blomqvist and Larsson, 1994). However, only 10% to
362 60% of the total vertical mass flux may be composed of primary organic carbon, while the remainder
363 has been interpreted as resuspended material (Blomqvist and Larsson, 1994).

364 A second effect to be considered is that stations B1 and H6 are located in bathymetric depressions. H6
365 is in the center of a sub-basin separated from the outer Himmerfjärd by a sill (Fig. 1). Likewise, Station
366 B1 is located in a small depression at the head of a submarine channel that opens to the Baltic Sea.
367 Fine-grained and reworked organic-rich material preferentially accumulates in these depressions
368 (Jonsson et al., 2003). Because of the importance of resuspended organic material for the vertical mass
369 flux and bioturbation, the annual variability in the organic matter composition at the sediment surface
370 varies year-round only between 5 and 6 % OC with relatively constant C/N ratios between 7.9 and 9.1
371 at Station B1 and 8.3 and 9.2 at Station H6 (Bonaglia et al., 2014). The combined effect of the
372 sedimentation characteristics is that temporal variability in the bottom settling primary organic carbon
373 flux is low, which reduces the overall temporal variability in organic carbon amount and composition
374 and thereby in carbon mineralization rates. This small temporal variability is further influenced by
375 macrofauna bioturbation in the top 5 cm of sediment in this area, foremost by the bivalve *Macoma*
376 *baltica*, the arthropod *Pontoporeia femorata*, and the polychaete *Marenzelleria* (Bonaglia et al., 2014).



377 Although macrofauna is largely absent at Station H6, sediment is also mixed at station H6 by
378 bioturbating meiofauna (mostly ostracods) (Bonaglia et al., 2014).
379 The measured benthic oxygen uptake rates are consistent with the low variability in the surface organic
380 carbon concentrations, C/N ratios, and a temperature-dependent decrease in total oxygen uptake rates in
381 winter. The slightly higher total oxygen uptake rate at Station H6 is also consistent with the
382 physiography of the enclosed small basin favouring sediment trapping of fine material. In addition, the
383 location of station H6 in the inner fjärd limits water exchange and leads to greater oxygen depletion,
384 whereas the more open station B1 is affected by upwelling of oxygen-rich waters and comparatively
385 less burial of organic material (Table 1).

386

387 **4.3 Methane fluxes, sulfate reduction and methane oxidation**

388 The inner Himmerfjärden sediments have very high sedimentation rates between 0.9 and 1.3 cm/yr
389 (Thang et al., 2013; Bianchi et al., 2002). In such sediments organic carbon burial and transfer of
390 organic matter into the methanogenic zone is efficient and will occur within 20 to 30 years. As a
391 consequence of the low salinity (< 6 ‰) of the Baltic Sea at this latitude, seawater sulfate
392 concentrations are less than 7 mM and, by comparison with normal seawater, a comparatively lesser
393 amount of organic matter can be degraded by bacterial sulfate reduction (Thang et al., 2013).
394 Consequently, compared to normal marine sediment a larger proportion of organic matter undergoes
395 anaerobic microbial degradation terminating in methanogenesis, which generates a high upward flux of
396 methane into the sulfate-containing zone. Organoclastic sulfate-reducing bacteria will compete for the
397 available sulfate with sulfate-reducing bacteria involved in the anaerobic oxidation of methane (Dale et
398 al., 2006; Jørgensen and Parkes, 2010). Thermodynamic and kinetic constraints decide on the outcome
399 between these two competing processes. Dale et al. (2006) suggested that due to lower winter
400 temperatures and greater sulfate availability in the sulfate-methane transition zone in winter, the
401 thermodynamic driving force for anaerobic methane oxidation increases allowing for a greater
402 proportion of anaerobic methane oxidation coupled to sulfate reduction in the winter. In the summer



403 and fall, higher temperatures and sulfate limitation favor organoclastic sulfate reduction and
404 methanogenesis while limiting the anaerobic oxidation of methane. Most importantly, however, their
405 analysis showed that due to thermodynamic constraints and slow growth rates of the methane-oxidizing
406 archaea the microbial biomass does not change significantly over a year. These conceptual modelling
407 results can be tested with our Himmerfjärden data.

408 Sulfate reduction rates, particularly at H6, demonstrate how strongly bottom-water oxygen controls
409 organic matter mineralization. In the spring, summer, and fall sulfate reduction was at its maximum in
410 the first two centimeters of the sediments (Fig 3 e, f, g). In February, reduced organic carbon input and
411 higher oxygen concentrations resulted in lower sulfate reduction rates and a shift of the maximum rates
412 to greater depths in the sediments (Figure 3 h). Since other terminal carbon-oxidizing processes (e.g.
413 denitrification, iron, and manganese reduction) outcompete sulfate reduction for electron-donating
414 substrates, the depth of sulfate penetration and organic matter degradation via sulfate shifts deeper in
415 the sediment which reduces methane production.

416 The decrease in oxygen uptake matches well with the decrease in methane fluxes at the two stations in
417 winter, which suggests an impact of oxygen on methane cycling (Table 2, Figure 5). Higher oxygen
418 levels enhance bioturbation and oxygen uptake by the abundant macro- and meiofauna (Norkko et al.,
419 2015), but the mixing of sediment also affects methane transport to the water column, as the main
420 transport process shifts from diffusion to advection. This effect is likely the main cause for the winter
421 decrease in methane fluxes and concentrations. More aerated conditions indirectly enhance methane
422 removal by sustaining aerobic methanotrophs (Valentine 2011). It is plausible that, as in other brackish
423 coastal sediments, aerobic methanotrophs at the surface of Himmerfjärden sediments consume a
424 significant part of upward-diffusing methane that was not oxidized by anaerobic methane oxidation
425 (McDonald et al 2005, Moussard et al 2009, Treude et al 2005a).

426 Published benthic methane fluxes for estuaries with similar salinities have a reported range of 0.002 to
427 0.25 mmol m⁻² d⁻¹ (Abril and Iversen, 2002; Martens and Klump, 1980; Sansone et al., 1998; Zhang et
428 al., 2008; Borges and Abril, 2012; Martens et al., 1998). The methane fluxes derived from our core



429 incubations ($0.1\text{--}2.6\text{ mmol m}^{-2}\text{ d}^{-1}$, ignoring the potentially biased value of $19.9\text{ mmol m}^{-2}\text{ d}^{-1}$) were
430 high compared to these published fluxes. Our fluxes are consistent with fluxes based on porewater
431 gradients by Thang et al. (2013) that were between 0.3 and $1.1\text{ mmol m}^{-2}\text{ d}^{-1}$ at 3 nearby stations
432 measured in May 2009.

433 A conspicuous property of all porewater profiles at station H6, with the exception of the February 2013
434 sampling period, was the absence of a concave upward curvature in the methane concentration profiles,
435 which would be expected for net methane oxidation by aerobic and anaerobic methane oxidation
436 (Martens et al., 1998). Most concentration profiles of sulfate and methane at Station H6 overlapped
437 without a significant change in the methane concentration gradient. A similar observation has been
438 made earlier for other Himmerfjärden sediments (Thang et al., 2013), and has also been reported for
439 sediments of the northwestern Black Sea shelf (Knab et al., 2009) and in organic-rich shelf sediment of
440 the Namibian upwelling system (Brüchert et al., 2009). Inefficient methane oxidation is also evident
441 from the diffusive fluxes, which showed that the upward fluxes of methane into the sulfate-methane
442 transition zone were only marginally higher than the methane fluxes to the sediment surface indicating
443 little attenuation of the methane flux in the sulfate-methane transition zone (Table 2). One possible
444 explanation for this phenomenon is therefore that rates of sulfate reduction–coupled anaerobic methane
445 oxidation, except for the winter months, were low compared to the total sulfate reduction rate. An
446 alternative explanation of our observations could be that the methane concentration gradients were
447 affected by the presence of rising methane bubbles (Haeckel et al., 2007), or that bioturbation and
448 bioirrigation linearized the concentration profiles (Dale et al., 2013). However, we do not favor this
449 interpretation because of the absence of large macrofauna at station H6 and the fast porewater methane
450 sampling method.

451 An analysis of the cumulative distribution of ^{35}S -SRR with depth at station H6 provides clues to the
452 proportion of organoclastic relative to anaerobic methane oxidation-coupled sulfate reduction at Station
453 H6 (Figure 6 e-h). The gradient in organoclastic sulfate reduction is well described by an exponential
454 law



455 $^{35}\text{SRR} = y z^{-b}$ (6)

456 where z is depth (cm) and y and b are regression coefficients (Jørgensen and Parkes, 2010). For the
457 sediments investigated here, the exponential coefficient b varied between 0.4 and 0.9 at station B1 and
458 0.3 and 0.8 at Station H6 (Table 4). At Station H6 the lowest coefficient was found for February 2013,
459 when sulfate penetrated the deepest into the sediment. Since the upward flux of methane provides an
460 additional energy source to sulfate-reducing bacteria, sulfate reduction rates are expected to increase in
461 the sulfate-methane transition zone. The net effect of a substantial AOM contribution to total sulfate
462 reduction is a low exponential coefficient b because the depth gradient in the sulfate reduction rate is
463 reduced. The difference between the exponential coefficients of the different sampling periods can be
464 used to calculate the variation in the contribution of AOM to the total sulfate reduction rate. At station
465 H6, between 5 % (August 2012) and 20% (April 2012) of the total sulfate reduction can be associated
466 with anaerobic methane oxidation. A comparison of the above method with the integrated ^{35}S -sulfate
467 reduction rates integrated over the H6 sediment cores with the rates integrated over the AOM zone also
468 indicated that >20% of sulfate respiration at H6 was fuelled by methane (Table 2). In near-shore
469 continental margin sediments worldwide, the fraction of methane-driven sulfate reduction varies
470 between locations and accounts for 3-40% of total SRR, with 10% possibly representing a global mean
471 value (Jørgensen and Kasten, 2006). The average 20% contribution calculated here falls in the upper
472 range of these values and is similar to values reported before for one of the monitoring stations within
473 Himmerfjärden (Thang et al., 2013) and also for a very productive Chilean slope sediment (8-24 %)
474 (Treude et al 2005b). The good match between the upward fluxes of methane in the sulfate-methane
475 transition zone and the measured sulfate reduction rates in the transition also indicate that other
476 proposed electron acceptors for anaerobic methane oxidation such as iron are unimportant in these
477 sediments (Beal et al., 2009; Egger et al. 2014).

478



479 **4.4 Temporal variability in hydrostatic pressure**

480 The abrupt decrease in porewater methane concentrations from November 2012 to late January/early
481 February 2013 and the subsequent increase in April 2013 cannot be explained by variation in methane
482 oxidation alone, because the temporal change in porewater methane concentration was large compared
483 to the inferred methane oxidation rates based on fluxes in and out of the AOM zone. In addition, except
484 for downward-diffusing sulfate, there was no significant other electron acceptor present at depth. It is
485 unlikely that rates of methanogenesis would have decreased significantly between the fall and the
486 winter and resumed again in the spring, because the sediment temperatures were similar in February
487 and April (Table 1). Changes in organic matter sedimentation at the sediment surface also have no
488 significant influence on methanogenesis in buried sediment and cannot explain the sudden decrease in
489 methane concentration at depth. An alternative explanation for the changes in methane concentrations
490 is required. A possible explanation could be that changes in upward transport of methane changes are
491 due to variability in hydrostatic pressure and the associated diffusive and advective upward transport of
492 methane from depth. The free gas depth of methane is thought to follow changes in hydrostatic pressure
493 and temperature (Mogollon et al., 2011; Toth et al., 2015). An estimated 10% of the fine-grained
494 sediments in the Stockholm archipelago area is underlain by pockets of free methane (Persson and
495 Jonsson, 2000) and these free gas pockets are preferentially located in areas with the thickest
496 postglacial mud accumulation, generally in the center of the sub-basins and along fault lineaments
497 (Söderberg and Floden, 1992). Based on sub-bottom echosounder profiling, the surface of the free gas
498 zone in accumulation areas in Himmerfjärden is between 1 and 3 meter depth. During low sealevel
499 stand the free gas zone is expected to migrate closer to the sediment surface, whereas during high
500 sealevel the free gas zone is depressed into the sediment. The total variation in sealevel may as much as
501 50 cm, sufficient to explain the changes in methane concentrations observed here. Unfortunately, data
502 on sealevel fluctuation is not available for our respective sampling locations, and general sealevel
503 stands should not be directly applied to the sample sites.

504



505 **5 Conclusions**

506 A greater understanding of methane emissions from estuarine and coastal sediments is important to
507 estimate the contribution of these environments to global marine methane fluxes. High benthic fluxes
508 of methane from these sediments showed that aerobic and anaerobic methane oxidation rates are
509 relatively inefficient, while still contributing up to 20% to total sulfate reduction. Higher bottom water
510 oxygen concentrations in winter played a pivotal role in methane removal in these sediments. Of the
511 different environmental regulators, bottom water oxygen had the strongest influence for the regulation
512 of methane emissions. Oxygen availability directly enhanced aerobic organic matter mineralization by
513 shifting the redox cascade in the sediments and indirectly by stimulating meiofauna and macrofauna
514 activity thereby stimulating both the aerobic carbon mineralization and oxidative recycling of sulfate.
515 The annual variability in sediment methane concentrations and benthic methane fluxes indicate that the
516 annual environmental changes at these near-shore, but relatively deep-water localities are considerable.
517 Very few data on sediment biogeochemical processes are currently available for aerobic and anaerobic
518 carbon mineralization and methane cycling during winter months when ice cover inhibits access and
519 sampling. Process rates inferred from sampling during open-water conditions over the whole year are
520 therefore likely overestimates. In addition, advective recharge of subsurface methane should also be
521 considered as an important transport component in deeper near-shore waters.

522

523



524 **6. Author contribution**

525 Joanna E. Sawicka conducted the sampling and analysis for the study and wrote the manuscript. Volker
526 Brüchert devised the study, interpreted the data, created the figures and tables, and wrote the
527 manuscript.

528

529 **7. Data availability**

530 The data are available from the second author upon request.

531

532 **8. Acknowledgments**

533 We are grateful to the staff of Askö Laboratory for their help and cooperation during the cruises and
534 our stays on the island of Askö. We would like to thank Barbara Deutsch, Camilla Olsson and Stefano
535 Bonaglia for their help during sampling. The study was funded by the grant from the Bolin Centre for
536 Climate Research, Baltic Ecosystem Adaptive management (BEAM), and the EU BONUS project
537 Baltic Gas.

538

539

540 **References**

- 541 Abril, G. and Iversen, N.: Methane dynamics in a shallow non-tidal estuary (Randers Fjord, Denmark), *Mar Ecol Prog Ser*,
 542 230, 171-181, 2002.
- 543 Amouroux, D., Roberts, G., Rapsomanikis, S. and Andreae, M.O.: Biogenic gas (CH₄, N₂O, DMS) emission to the
 544 atmosphere from near-shore and shelf waters of the North-western Black Sea, *Estuar Coast Shelf S*, 54, 575-587,
 545 2002.
- 546 Bange, H. W., Bergmann, K., Hansen, H. P., Kock, A., Koppe, R., Malien, F., Ostrau, F., Dissolved methane during hypoxic
 547 events at the Boknis Eck time series station (Eckernförde Bay, SW Baltic Sea), *Biogeosciences*, 7, 1279-1284,
 548 2010.
- 549 Beal, E. J., House, C. H., Orphan, V. J.: Manganese- and Iron-Dependent Marine Methane Oxidation, *Science* 325, 184-
 550 187, 2009.
- 551 Bianchi, T. S., Engelhaupt, E., McKee B. A., Miles, S., Elmgren, R., Hajdu, S., Savage, C., and Baskaran, M.: Do sediments
 552 from coastal sites accurately reflect time trends in water column phytoplankton? A test from Himmerfjärden Bay
 553 (Baltic Sea proper), *Limnol. Oceanogr.*, 47, 1537-1544, 2002.
- 554 Blomqvist, S. and Larsson, U.: Detrital bedrock elements as tracers of settling resuspended particulate matter in a coastal
 555 area of the Baltic Sea, *Limnol. Oceanogr.*, 39, 880-896, 1994.
- 556 Boesch, D. F., Hecky, R., O'Melia, C., Schindler, D., Seitzinger, S.: Eutrophication of the Swedish Seas, Reports of the
 557 Swedish Environmental Protection Agency, Stockholm, Sweden, No. 5509, 72 p, 2006.
- 558 Bonaglia, S., Bartoli, M., Gunnarsson, J. S., Rahm, L., Raymond, C., Svensson, O., Shakeri, Brüchert, V.: Effect of
 559 reoxygenation and *Marenzelleria* spp. bioturbation on Baltic Sea sediment metabolism, *Marine Ecology Progress*
 560 *Series*, 482, 43-55, 2013.
- 561 Bonaglia, S., Deutsch, B., Bartoli, M., Marchant, H. K. and Brüchert, V.: Seasonal oxygen, nitrogen and phosphorus benthic
 562 cycling along an impacted Baltic Sea estuary: regulation and spatial patterns, *Biogeochemistry*, 119, 1-22, 2014.
- 563 Borges, A. V. and Abril, G.: Carbon Dioxide and Methane Dynamics in Estuaries, in: *Treatise on Estuarine and Coastal*
 564 *Science*, (Eds.) Wolanski, E., McLusky, D., Academic Press, Waltham, 119-161, 2011.
- 565 Boudreau, B.P.: *Diagenetic models and their implementation*. Springer Verlag, Berlin Heidelberg, 1996.
- 566 Brüchert, V., Currie, B., Peard, K.: Hydrogen sulphide and methane emissions on the central Namibian shelf, *Progr.*
 567 *Oceanogr.*, 83, 169-179, 2009.
- 568 Crill, P. M. and Martens, C. S.: Spatial and temporal fluctuations of methane production in anoxic coastal marine sediments,
 569 *Limnol. Oceanogr.*, 6, 1117-1130, 1983.
- 570 Dale, A. W., Regnier, P., Van Cappellen, P.: Bioenergetic Controls on Anaerobic Oxidation of Methane (AOM) in Coastal
 571 Marine Sediments: A Theoretical Analysis, *Am. J. Sci.*, 306, 246-294, 2006.
- 572 Dale, A. W., Aguilera, D. R., Regnier, P., Fossing, H., Knab, N. J., Jørgensen, B. B.: Seasonal dynamics of the depth and
 573 rate of anaerobic oxidation of methane in Aarhus Bay (Denmark) sediments, *J. Mar. Res.*, 66, 127-155, 2008.
- 574 Dale, A. W., Bertics, V. J., Treude, T., Sommer, S., Wallmann, K.: Modeling benthic-pelagic nutrient exchange processes
 575 and porewater distributions in a seasonally hypoxic sediment: evidence for massive phosphate release by
 576 *Beggiatoa*? *Biogeosciences*, 10, 629-651, 2013.
- 577 Egger, M., Rasigraf, O., Sapart, C. J., Jilbert, T., Jetten, M. S. M., Röckmann, T.: Iron-mediated anaerobic oxidation of
 578 methane in brackish coastal sediments, *Env. Sci. Technol.*, 49, 277-283, 2014.
- 579 Elmgren, R. and Larsson, U.: Himmerfjärden: förändringar i ett näringsbelastat kustekosystem i Östersjön, Reports of the
 580 Swedish Environmental Protection Agency, Stockholm, Sweden, 1997.
- 581 Engqvist, A., Long-term nutrient balances in the eutrophication of the Himmerfjärden, *Estuar. Coast. Shelf S.*, 42, 483-507,
 582 1996.
- 583 Haeckel, M., Boudreau, B. P., Wallmann, K.: Bubble-induced porewater mixing: A 3-D model for deep porewater
 584 irrigation, *Geochim Cosmochim. Acta*, 71, 5135-5154, 2007.
- 585 Harvey, E. T., Kratzer, S., Philipson, P.: Satellite-based water quality monitoring for improved spatial and temporal retrieval
 586 of chlorophyll-a in coastal waters, *Remote Sens. Environ.*, 158, 417-430, 2015.
- 587 Iversen, N., Jørgensen, B. B.: Diffusion coefficients of sulfate and methane in marine sediments: Influence of porosity,
 588 *Geochim. Cosmochim. Acta* 57, 571-578, 1994.
- 589 Jørgensen, B. B. and Kasten, S.: Sulfur Cycling and Methane Oxidation, In: *Marine Geochemistry*, (Eds.) Schulz H. and
 590 Zabel, M., Springer, Berlin Heidelberg, 271-309, 2006.
- 591 Jørgensen, B. B.: A comparison of methods for the quantification of bacterial sulfate reduction in coastal marine sediments,
 592 *Geomicrobiol. J.*, 1, 11-27, 1978.



- 593 Jørgensen, B. B. and Parkes, R. J.: Role of sulfate reduction and methane production by organic carbon degradation in
 594 eutrophic fjord sediments (Limfjorden, Denmark), *Limnol. Oceanogr.*, 55, 1338-1352, 2010.
- 595 Jonsson, P., Persson, J., Holmberg, P.: Skärgårdens bottnar, Report of the Swedish Environmental Protection Agency,
 596 Stockholm, No. 5212, 114, 2003.
- 597 Kallmeyer, J., Ferdelman, T. G., Weber, A., Fossing, H., Jørgensen, B. B.: Evaluation of a cold chromium distillation
 598 procedure for recovering very small amounts of radiolabeled sulfide related to sulfate reduction measurements,
 599 *Limnol. Oceanogr. Meth.*, 2, 171-180, 2004.
- 600 Kampbell, D. H., Wilson, J. T., Vandegrift, S. A.: Dissolved Oxygen and Methane in Water by a GC Headspace
 601 Equilibration Technique, *Intern. J. Environ. An. Ch.*, 36, 249-257, 1989.
- 602 Knab, N. J., Cragg, B. A., Borowski, C., Parkes, R. J., Pancost, R. and Jørgensen, B. B.: Anaerobic oxidation of methane
 603 (AOM) in marine sediments from the Skagerrak (Denmark): I. Geochemical and microbiological analyses.
 604 *Geochim. Cosmochim. Acta*, 72, 2868-2879, 2009.
- 605 Knittel, K. and Boetius, A.: Anaerobic Oxidation of Methane: Progress with an Unknown Process. *Ann. Rev. Microbiol.*,
 606 63: 311-334, 2009.
- 607 Klump, J. V. and Martens, C. S.: Biogeochemical cycling in an organic rich coastal marine basin—II. Nutrient sediment-
 608 water exchange processes. *Geochim. Cosmochim. Acta*, 45, 101-121, 1981.
- 609 Kristensen, E., Bouillon, S., Dittmar, T., Marchand, C.: Organic carbon dynamics in mangrove ecosystems: A review.
 610 *Aquat. Bot.*, 89, 201-219, 2008.
- 611 Leloup, J., Fossing, H., Kohls, K., Holmkvist, L., Borowski, C., Jørgensen, B. B.: Sulfate-reducing bacteria in marine
 612 sediment (Aarhus Bay, Denmark): abundance and diversity related to geochemical zonation. *Environ. Microbiol.*,
 613 11, 1278-1291, 2009.
- 614 Martens, C. S., Albert, D. B., Alperin, M. J.: Biogeochemical processes controlling methane in gassy coastal sediments -
 615 Part I. A model coupling organic matter flux to gas production, oxidation, and transport. *Cont. Shelf Res.*, 18,
 616 1741-1770, 1998.
- 617 Martens, C. S. and Berner, R. A.: Methane production in the interstitial waters of sulfate-depleted marine sediments.
 618 *Science*, 185, 1167-1169, 1974.
- 619 Martens, C. S. and Klump, J.: Biogeochemical cycling in an organic-rich coastal marine basin. 4. An organic carbon budget
 620 for sediments dominated by sulfate reduction and methanogenesis. *Geochim. Cosmochim. Acta*, 48, 1987-2004,
 621 1984.
- 622 Martens, C.S. and Val Klump, J.: Biogeochemical cycling in an organic-rich coastal marine basin—I. Methane sediment-
 623 water exchange processes. *Geochim. Cosmochim. Acta*, 44, 471-490, 1980.
- 624 Marty, D., Bonin, P., Michotey, V. and Bianchi, M.: Bacterial biogas production in coastal systems affected by freshwater
 625 inputs. *Cont. Shelf Res.*, 21, 2105-2115, 2001.
- 626 McDonald, I. R., Smith, K., Lidstrom, M. E.: Methanotrophic populations in estuarine sediment from Newport Bay,
 627 California, *FEMS Microbiol. Lett.*, 250, 287-293, 2005.
- 628 Middelburg, J., Nieuwenhuize, J., Iversen, N., Høgh, N., de Wilde, H., Helder, W., Seifert, R. and Christof, O.: Methane
 629 distribution in European tidal estuaries, *Biogeochemistry*, 59, 95-119, 2002.
- 630 Mogollón, J. M., Dale, A. W., L'Heureux, I., Regnier, P.: Impact of seasonal temperature and pressure changes on methane
 631 gas production, dissolution, and transport in unfractured sediments, *J. Geophys. Res. Biogeosci.*, 116, G03031,
 632 2011.
- 633 Moussard, H., Stralis-Pavese, N., Bodrossy, L., Neufeld, J. D., Murrell, J. C.: Identification of active methylotrophic
 634 bacteria inhabiting surface sediment of a marine estuary, *Environ. Microbiol. Repts.*, 1, 424-433, 2009.
- 635 Musenze, R.S., Werner, U., Grinham, A., Udy, J. and Yuan, Z.: Methane and nitrous oxide emissions from a subtropical
 636 estuary (the Brisbane River estuary, Australia), *Sci. Total Environ.*, 472, 719-729, 2014.
- 637 Norkko, J., Gammal, J., Hewitt, J., Josefson, A., Carstensen, J., Norkko, A.: Seafloor Ecosystem Function Relationships: In
 638 Situ Patterns of Change Across Gradients of Increasing Hypoxic Stress, *Ecosystems* 18, 1424-1439, 2015.
- 639 Persson, J., Jonsson, P.: Historical development of laminated sediments—an approach to detect soft sediment ecosystem
 640 changes in the Baltic Sea. *Mar. Poll. Bull.*, 40, 122-134, 2000.
- 641 Reeburgh, W. S.: Oceanic Methane Biogeochemistry, *Chem. Rev.*, 107, 486-513, 2007.
- 642 Reindl, A. R. and Bolałek, J.: Methane flux from sediment into near-bottom water and its variability along the Hel
 643 Peninsula—Southern Baltic, Sea, *Cont. Shelf Res.*, 74, 88-93, 2014.
- 644 Savage, C., Leavitt, P. R., Elmgren, R.: Effects of land use, urbanization, and climate variability on coastal eutrophication in
 645 the Baltic Sea. *Limnol. Oceanogr.*, 55, 1033-1046, 2010.



- 646 Sansone, F. J., Holmes, M. E. and Popp, B. N.: Methane stable isotopic ratios and concentrations as indicators of methane
647 dynamics in estuaries. *Global Biogeochem. Cycles*, 13, 463-474, 1999.
- 648 Sansone, F. J., Rust, T. M. and Smith, S. V., 1998. Methane Distribution and Cycling in Tomales Bay, California, *Estuaries*,
649 21, 66-77.
- 650 Seeberg-Elverfeldt, J., Schlüter, M., Feseker, T., Kölling, M.: Rhizon sampling of porewaters near the sediment-water
651 interface of aquatic systems. *Limnol. Oceanogr. Meth.*, 3, 361-371, 2005.
- 652 Smith, R.W., Bianchi, T.S., Allison, M., Savage, C., Galy, V.: High rates of organic carbon burial in fjord sediments
653 globally. *Nature Geosci.*, 8, 450-453, 2015.
- 654 Söderberg, P. and Flodén, T.: Gas seepages, gas eruptions and degassing structures in the seafloor along the Strömna
655 tectonic lineament in the crystalline Stockholm Archipelago, east Sweden. *Cont. Shelf Res.* 12, 1157-1171, 1992.
- 656 Thang, N., Brüchert, V., Formolo, M., Wegener, G., Ginters, L., Jørgensen, B. B., and Ferdelman, T.: The Impact of
657 Sediment and Carbon Fluxes on the Biogeochemistry of Methane and Sulfur in Littoral Baltic Sea Sediments
658 (Himmerfjärden, Sweden), *Estuaries and Coasts*, 36, 98-115, 2013.
- 659 Tóth, Z., Spiess, V., Keil, H.: Frequency dependence in seismoacoustic imaging of shallow free gas due to gas bubble
660 resonance, *J. Geophys. Res. Solid Earth*, 120, 8056-8072, 2015.
- 661 Treude, T., Krüger, M., Boetius, A., Jørgensen, B. B.: Environmental control on anaerobic oxidation of methane in the
662 gassy sediments of Eckernförde Bay (German Baltic), *Limnol. Oceanogr.*, 50, 1771-1786, 2005a.
- 663 Treude, T., Niggemann, J., Kallmeyer, J., Wintersteller, P., Schubert, C. J., Boetius, A., and Jørgensen, B. B.: Anaerobic
664 oxidation of methane and sulfate reduction along the Chilean continental margin, *Geochim. Cosmochim. Acta*, 69,
665 2767-2779, 2005b.
- 666 Upstill-Goddard, R. C., Barnes, J., Frost, T., Punshon, S. and Owens, N. J. P.: Methane in the southern North Sea: Low-
667 salinity inputs, estuarine removal, and atmospheric flux, *Global Biogeochem. Cycles*, 14, 1205-1217, 2000.
- 668 Valentine, D.L.: Emerging Topics in Marine Methane Biogeochemistry. *Annual Rev. Mar. Sci.*, 3, 147-171, 2011.
- 669 Wegener, G., Bausch, M., Holler, T., Thang, N. M., Prieto Mollar, X., Kellermann, M. Y., Hinrichs, K. U., and Boetius, A.:
670 Assessing sub-seafloor microbial activity by combined stable isotope probing with deuterated water and ¹³C-
671 bicarbonate. *Environ. Microbiol.*, 14, 1517-1527, 2012.
- 672 Westrich, J. T., Berner, R. A.: The role of sedimentary organic matter in bacterial sulfate reduction: The G model tested.
673 *Limnol. Oceanogr.*, 29, 236-249, 1984.
- 674 Wilhelm, E., Battino, R., and Wilcock, R. J.: Low-pressure solubility of gases in liquid water. *Chem. Rev.*, 77, 219-262,
675 1977.
- 676 Zakrisson, A., and Larsson, U.: Regulation of heterocyst frequency in Baltic Sea *Aphanizomenon* sp., *J. Plankton Res.*, 36,
677 1357-1367, 2014.
- 678 Zhang, G., Zhang, J., Liu, S., Ren, J., Xu, J. and Zhang, F.: Methane in the Changjiang (Yangtze River) estuary and its
679 adjacent marine area: riverine input, sediment release and atmospheric fluxes. *Biogeochemistry*, 91, 71-84, 2008.
- 680 Zhang, W., Bougouffa, S., Wang, Y., Lee, O. O., Yang, J., Chan C. Song, X., and Qian, P.-Y.: Toward understanding the
681 dynamics of microbial communities in an estuarine system, *PLoS ONE*, 9, e94449, 2014.
- 682



683 **Table 1.** Main site characteristics of the sampling stations.

Station	Sampling time	Water depth (m)	Temperature (°C)	Bottom water salinity (‰)	Bottom water Oxygen (µM)	Surface organic carbon (%)
B1 58°48'18"N 17°37'52"E	April 2012	41	2.4	6.5	160	6.0
	August 2012		6.9	7.0	260	5.2
	October 2012		6.8	7.0	224	5.1
	February 2013		3.4	7.0	380	5.0
H6 59°04'08"N 17°40'63"E	April 2012	39.5	1.8	5.9	40	4.6
	August 2012		6.7	6.4	150	5.1
	October 2012		9.4	6.5	191	5.2
	February 2013		1.8	5.4	300	4.7

684

685

686

687

688

689

690

691


 692 **Table 2.** Summary of CH₄ and SO₄²⁻ fluxes, depth-integrated ³⁵SRR, and total oxygen uptake (TOU).

Station	Sampling time	Flux (mmol m ⁻² d ⁻¹)						Integrated ³⁵ S-SRR (n=3)
		TOU whole core incubation (n=4)	CH ₄ whole core incubation (n=4)	CH ₄ Diffusive flux out of sediment (n=1)	CH ₄ Diffusive flux into SMTZ (n=1) ²	SO ₄ ²⁻ Diffusive flux into sediment (n=1)	³⁵ S-SRR integrated over AOM ³ zone (n=3)	
B1	April 2012	-19.7	1.2	1.6		-0.4	no AOM zone ⁴	-2.3
	August 2012	-22.5	1.2	no data		-0.8	no AOM zone ⁴	-0.5
	October 2012	-21.1	1.9	1.9		-1.3	no AOM zone ⁴	-2.0
	January 2013	-12.0	0.1	0.1		-0.2	no AOM zone ⁴	-2.2
H6	April 2012/13	-23.5	3.9 ¹	2.2	2.8	-2.6	(10-15 cm)=2.8	-11.6
	August 2012	-26.9	19.9 ⁵	2.4	2.6	-2.5	(10-15 cm)=2.8	-11.7
	October 2012	-25.9	1.8	1.8	1.9	-2.6	(10-15 cm)=2.4	-11.5
	January 2013	-14.9	1.7	0.1	0.4	-1.3	no AOM zone ³	-9.2

 693 ¹ whole core incubation was performed in April 2013; Diffusive fluxes were calculated for samples collected in April 2012;

 694 ² SMTZ - sulfate methane transition zone, ³ AOM zone – zone of anaerobic oxidation of methane, ⁴ no AOM zone means

 695 that AOM zone was probably deeper than the core length; ⁵ potentially elevated due to depressurization/ex-solution

696 effect during core incubation at atmospheric pressure;

697



698 **Table 3.** Best-fit regression coefficients a and b for the depth gradient of sulfate
699 reduction rates ($^{35}\text{SRR} = az^{-b}$ (z =depth, cm)).

Station	Sampling time	Exponential coefficient (a)	Exponential coefficient (b)
B1	April 2012	147.0	-1.4
	August 2012	11.7	-0.9
	October 2012	16.0	-0.4
	February 2013	33.5	-0.8
H6	April 2012	18.6	-0.5
	August 2012	37.4	-0.5
	October 2012	133.2	-0.8
	February 2013	25.0	-0.4

700

701



702

703

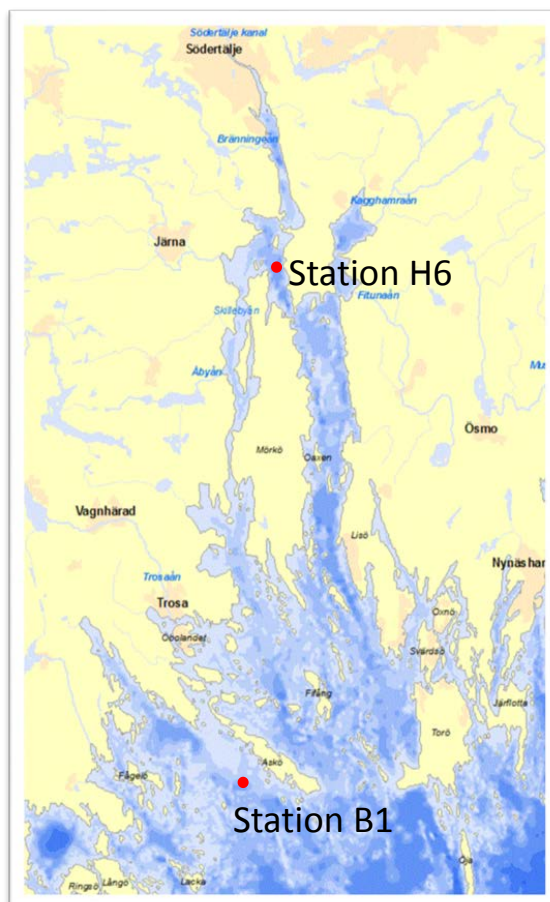
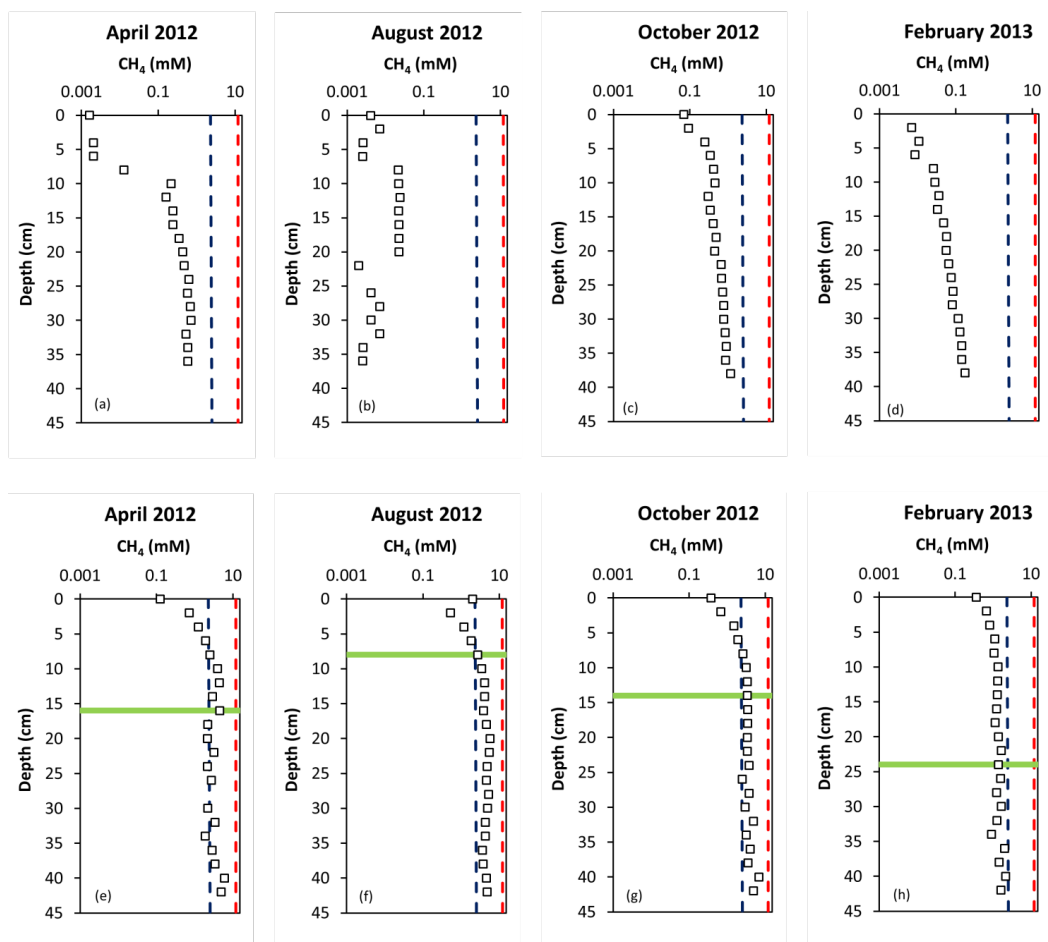


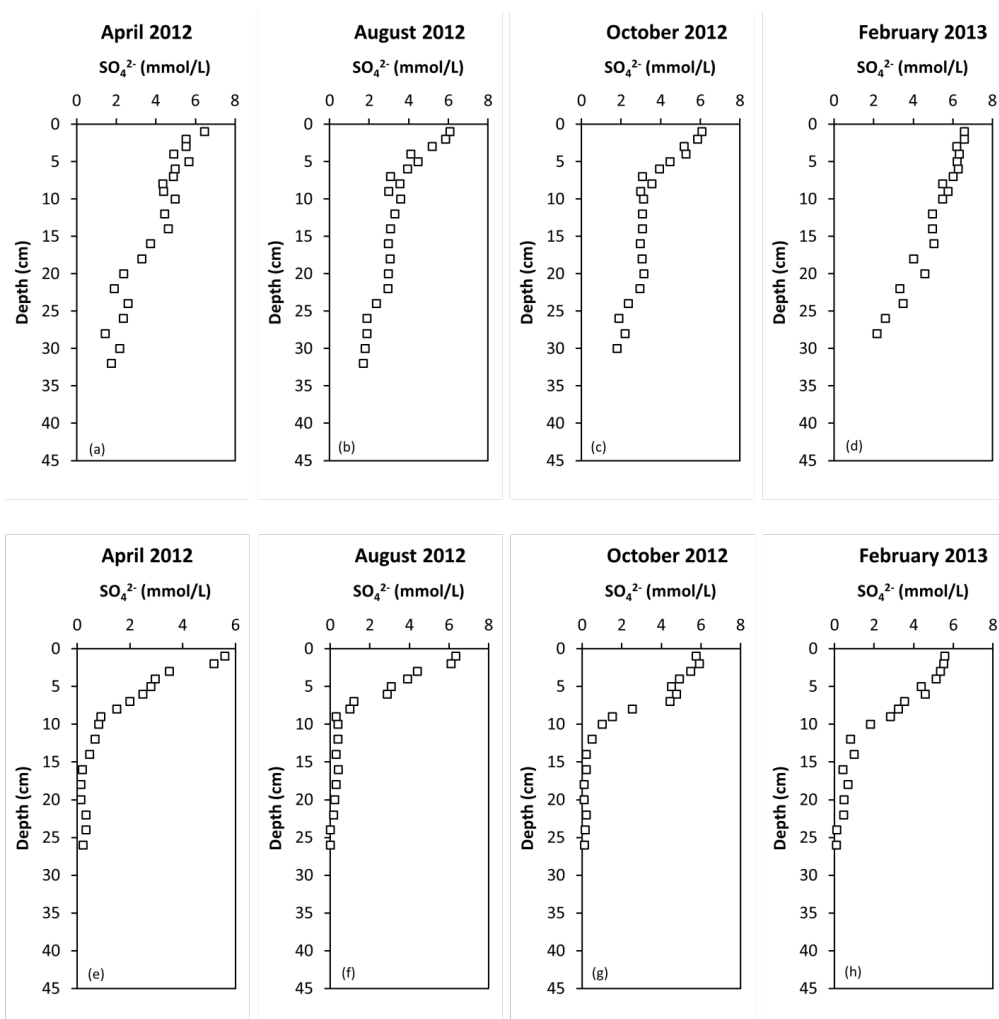
Figure 1. Location of sampling sites in Himmerfjärden, Stockholm Archipelago, Sweden. Detailed studies were conducted at two sites, an open water site (Station B1) and in the inner part of the estuary (Station H6).



704

705

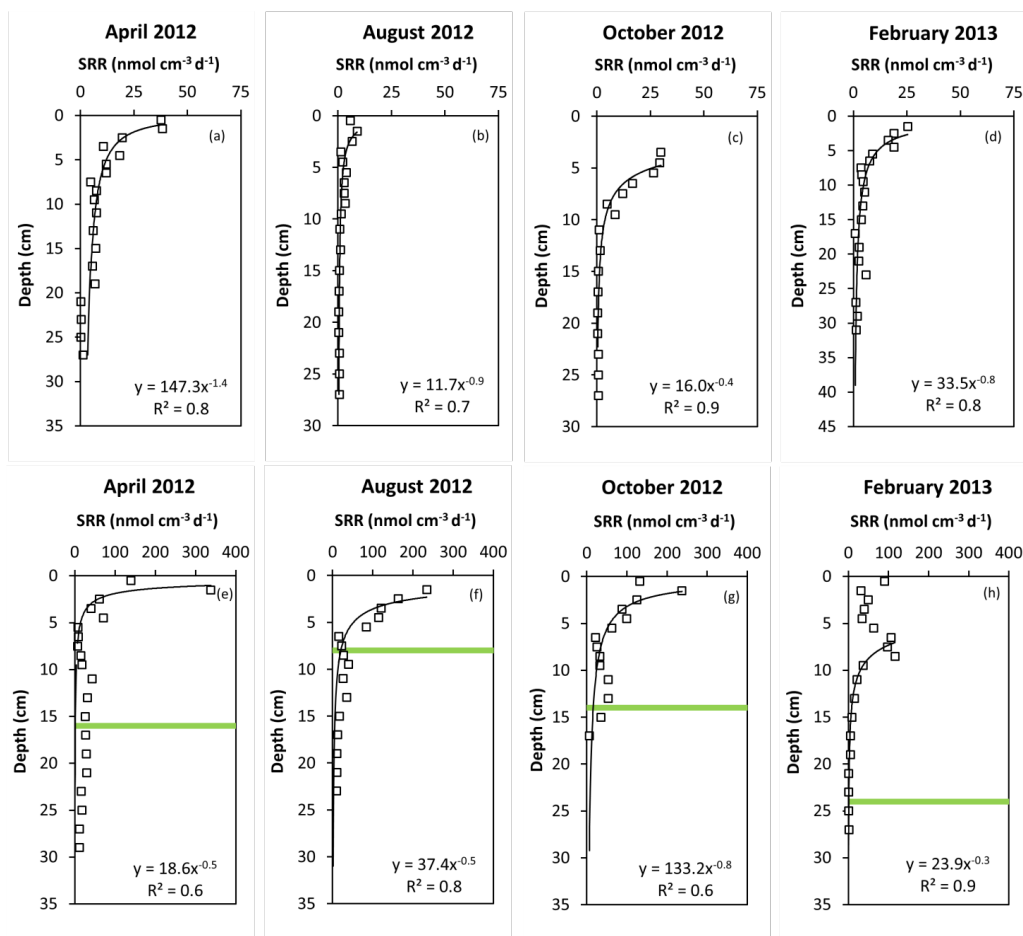
Figure 2. Porewater profiles of total methane at Station B1 (a-d) and Station H6 (e-h) for the different sampling periods. The green line marks the maximum depth of sulfate penetration. The dashed lines indicate the methane saturation concentration at 1 atm pressure (grey) and at the seafloor hydrostatic pressure (red) at the time of sampling.



706

707

Figure 3. Porewater profiles of dissolved sulfate at Station B1 (a-d) and Station H6 (e-h) for the different sampling periods.



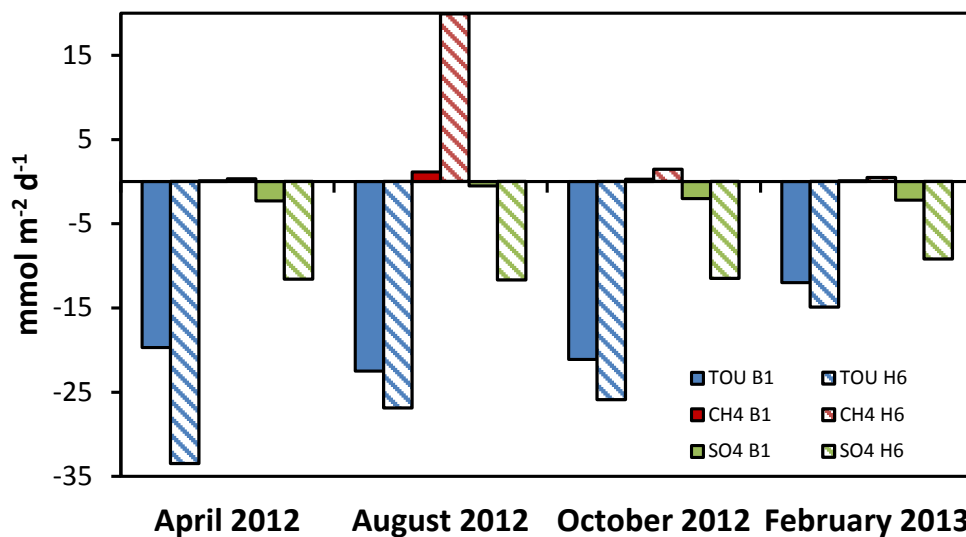
708

709

Figure 4. Depth gradients of bacterial sulfate reduction rates (SRR) measured with ³⁵S-sulfate. Black lines show the regression results to a power law of the form $y = ax^{-b}$. The green line marks the maximum depth of sulfate penetration.

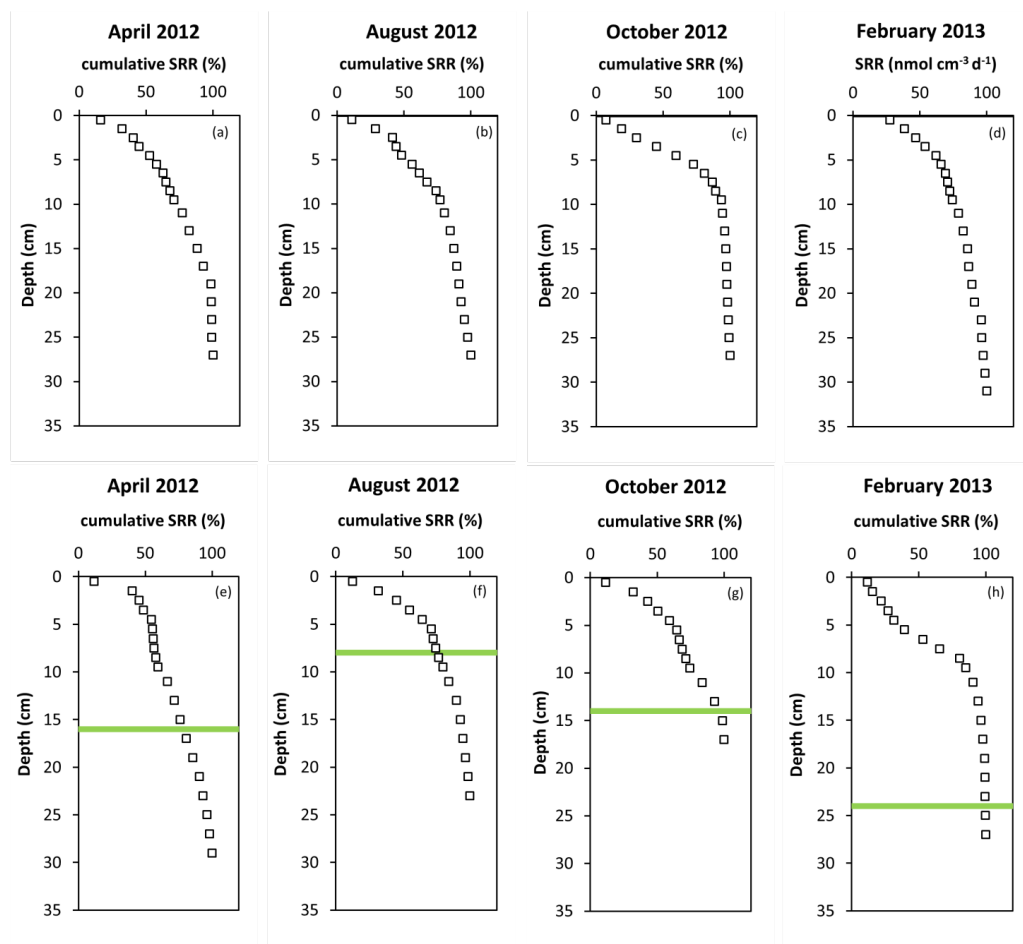


710



711

Figure 5. Comparison of benthic fluxes ($\text{mmol m}^{-2} \text{d}^{-1}$) for sulfate (SO_4), methane (CH_4), and oxygen for the different sampling periods.



712

Figure 6. Depth distribution of sulfate reduction rate expressed as cumulative percentage. The green line marks the maximum depth of sulfate penetration.